Supplementary Information: Enhanced glass dynamics facilitated by soft interfaces

Peng Luo,[1, a)] Zixuan Lin,[1] Kritika Jha,[1] Sarah E. Wolf,[2] Shivajee Govind,[1] Juliana I Bonilla Lugo,[1] Richard B. Stephens,[1, 3] and Zahra Fakhraai[1, b)]

[1)]*Department of Chemistry, University of Pennsylvania, Philadelphia, Pennsylvania, 19104, USA*

[2)]*Department of Chemistry, State University of New York Cortland, Cortland, New York, 13045, USA*

[3)]*Department of Physics, University of Pennsylvania, Philadelphia, Pennsylvania, 19104, USA*

This PDF file includes:

[a)]Corresponding Author: pengluo@iphy.ac.cn; Current Address: Institute of Physics, Chinese Academy of Sciences, Beijing 100190, China

[b)]Corresponding Author: fakhraai@sas.upenn.edu

SUPPLEMENTARY NOTE 1

Estimation of the average aging rate. Since the T_g of 50-nm-thick LQG layers on both soft and rigid substrates are the same as bulk T_g (**Supplementary Fig. 1**), their aging rates are expected to be similar to bulk samples. Furthermore, previous studies on polymer glasses have shown that the formation of a polymer/rubber interface does not affect the aging rate, even when the local T_g is substantially shifted[1, 2]. Therefore, the average rate of change of the LQG layer thickness due to aging ($\langle v_{ag} \rangle$) was estimated based on the aging studies by Cheng *et al.*[3] in bulk TPD LQGs (shown in **Supplementary Fig. 6**). For simplicity, it was assumed that the aging rate is constant over the experimental time window. While aging is not necessarily linear with time, $\langle v_{ag} \rangle$ was found to be much slower than dz_b/dt for most data points. As shown in **Supplementary Fig. 8**, adding $\langle v_{ag} \rangle$ to $\langle dz_b/dt \rangle$ did not make a significant difference in the estimated value of $\langle v_{gr,b} \rangle$, confirming that the rate of aging had a negligible effect on the calculation of growth front velocity.

SUPPLEMENTARY NOTE 2

Calculation of $\Delta\rho$, T_f, and birefringence. The relative density change, $\Delta\rho$, is determined from the average refractive indices ($\langle n \rangle$) measured before and after the thermal transformation of SG and bilayer films, using the Lorentz-Lorenz equation [4].

For optically anisotropic films ($n_{xy} \neq n_z$), $\langle n \rangle$ can be calculated as:

$$\langle n \rangle = \sqrt{\frac{{n_x}^2 + {n_y}^2 + {n_z}^2}{3}} = \sqrt{\frac{2{n_{xy}}^2 + {n_z}^2}{3}}. \tag{1}$$

The density of glass is correlated with its transparent refractive index through the Lorentz-Lorenz equation [4],

$$\frac{n^2 - 1}{n^2 + 2} = \frac{\alpha N_A \rho}{3\varepsilon_0 M_W}, \tag{2}$$

where ρ is density, α the molecular polarizability, N_A the Avogadro number, ε_0 the permittivity of the free space, and M_W the molecular molar mass. This equation indicates that n can be used as an independent measure of density without relying on thickness change upon film transformation. Our previous work [5] has demonstrated that this correlation holds for TPD glass films over a broad range of film thicknesses.

Assuming the changes in n and ρ are small, we have:

$$\frac{6n}{(n^2+2)^2} dn = \frac{\alpha N_A}{3\varepsilon_0 M_W} d\rho. \tag{3}$$

By dividing **Supplementary Eq. 3** by **Supplementary Eq. 2** we get the relative changes:

$$\frac{d\rho}{\rho} = \frac{6n^2}{(n^2+2)(n^2-1)}\frac{dn}{n}. \tag{4}$$

We define $\Delta\rho = (\rho - \rho_{\mathrm{LQG}})/\rho$, and $\Delta n = (n - n_{\mathrm{LQG}})/n$, to substitute for $d\rho/\rho$ and dn/n respectively, we have:

$$\Delta\rho = \frac{6n^2}{(n^2+2)(n^2-1)}\Delta n. \tag{5}$$

With **Supplementary Eq. 5** the relative density change ($\Delta\rho$) can be calculated using the relative change in the refractive index (Δn), compared to the values of LQG at 298 K. For birefringent samples, $\langle n \rangle$ is used instead of n.

The fictive temperature, T_{f}, is calculated based on the temperature dependence of $\Delta\rho$ for equilibrium SCL and SG[6]. Birefringence is defined as the difference between the out-of-plane (n_{z}) and in-plane (n_{xy}) refractive indices. A lower birefringence, indicated by a smaller absolute value, signifies a more isotropic molecular orientation in the glass.

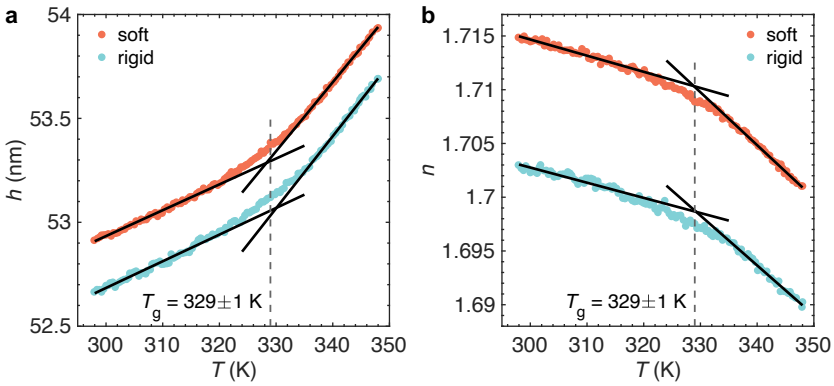

Supplementary Fig. 1 | T_g measurement for 50-nm-thick LQG films on soft and rigid substrates. **a**, Thickness, and **b**, refractive index at λ = 632.8 nm, as a function of temperature during cooling at 10 nm/min. The glass transition temperature, T_g, determined from the intersection of linear fits to the SCL and glass regions, is 329 ± 1 K, independent of substrate elasticity.

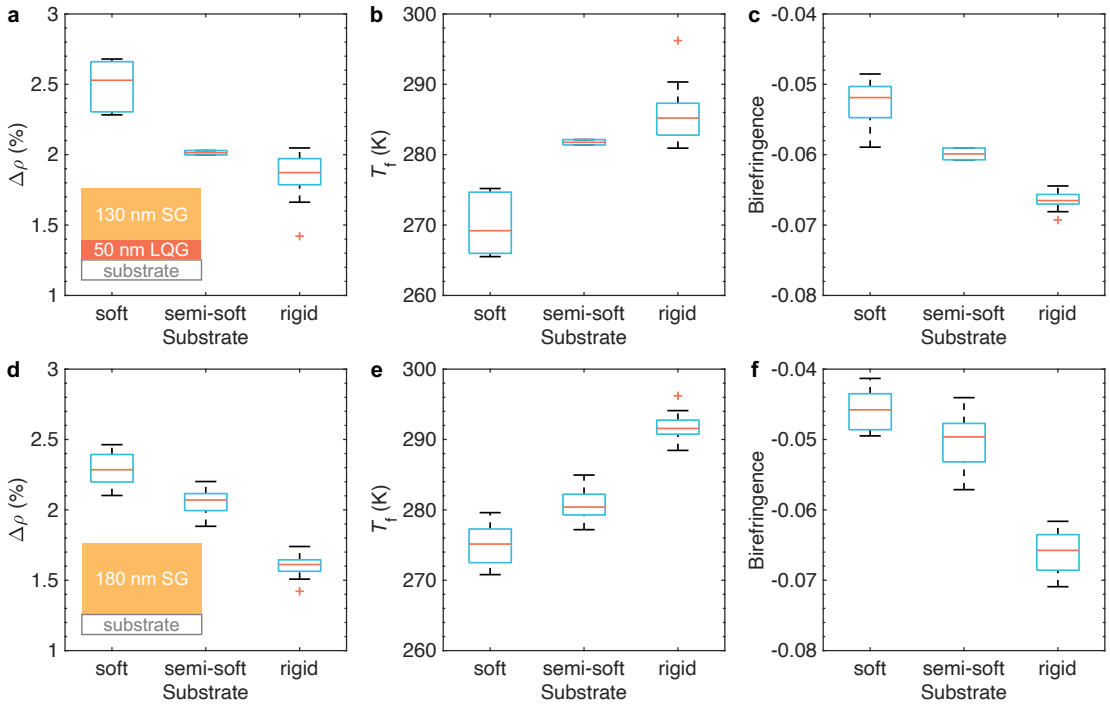

Supplementary Fig. 2 | Properties of the SG in bilayer and single-layer samples prepared on various substrates. a,**d**, Relative density change ($\Delta\rho$), **b**,**e**, fictive temperature (T_f), and **c**,**f**, birefringence, for 130-nm-thick SGs atop 50-nm-thick LQGs (**a**-**c**) and 180-nm-thick SGs (**d**-**f**). The boxplot center line represents the median, the boxes denote the interquartile ranges (IQR), whiskers extend to the minimum and maximum values within 1.5IQR, and outliers are marked as red crosses.

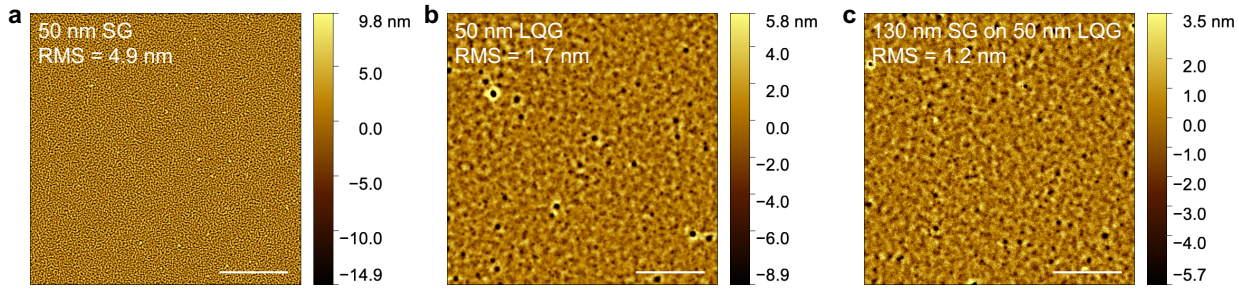

Supplementary Fig. 3 | Atomic force microscope (AFM) images of TPD glass films deposited on soft substrates. **a**, As-deposited 50-nm-thick SG film. **b**, LQG obtained by heating the same SG film in **a** to SCL state at 343 K for 10 minutes and quenching back to room temperature. **c**, A 130-nm-thick SG film deposited on a 50-nm-thick LQG layer. The scale bars for all images are 5 μm. Root-mean-square (RMS) roughness values are indicated on each image.

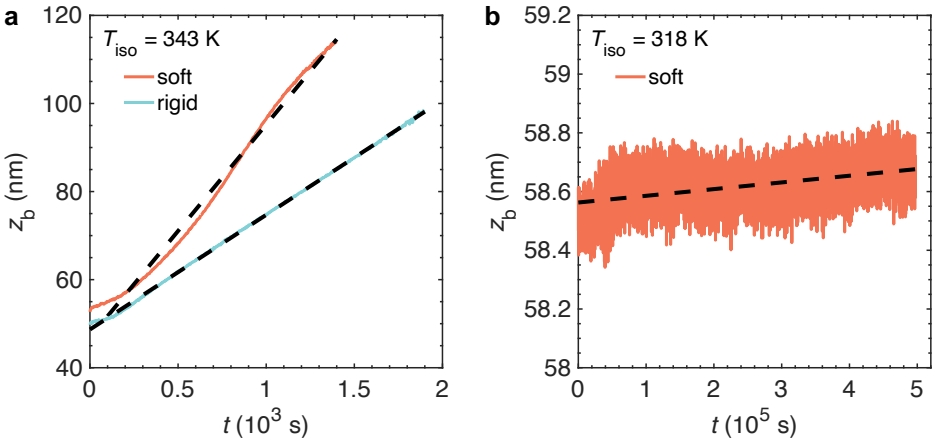

Supplementary Fig. 4 | Position of the buried SG/transformed-SCL interface, z_b, vs. time during isothermal annealing at two different T_{iso}: a, 343 K, and **b**, 318 K. The bilayer glasses were prepared on rigid and soft substrates. Dashed lines represent linear fits. The fitted slopes, *i.e.*, upward moving velocities ($\langle dz_b/dt \rangle$) are, $4.8 \times 10^{-2} \pm 2.3 \times 10^{-4}$ nm/s on soft substrate and $2.6 \times 10^{-2} \pm 1.9 \times 10^{-5}$ nm/s on rigid substrate at $T_{iso} = 343$ K, and $2.3 \times 10^{-7} \pm 3.3 \times 10^{-9}$ nm/s on soft substrate at $T_{iso} = 318$ K, respectively. Error bars represent the standard error of the regression parameters.

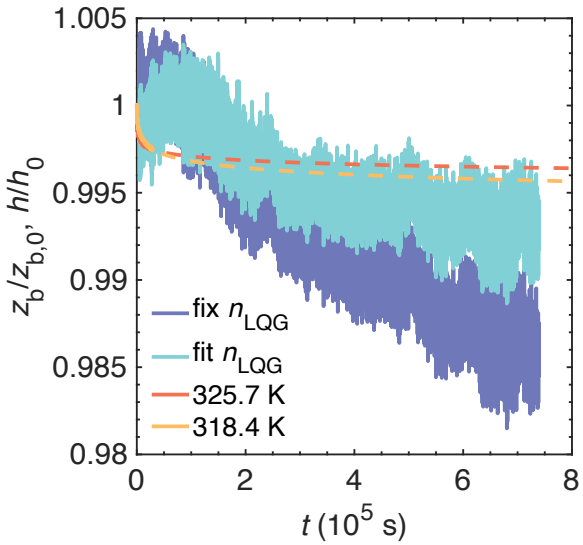

Supplementary Fig. 5 | Normalized position of the buried SG/LQG interface, $z_b/z_{b,0}$, vs. time during isothermal annealing at $T_{iso} = 323$ K, for a bilayer film prepared on rigid substrate. The two data represent results from two fitting approaches for the *in-situ* SE data: fixing the refractive index of the bottom LQG layer (n_{LQG}) or fitting it. The normalized thicknesses (h/h_0) of 400-nm-thick LQG films during aging at 325.7 K and 318.4 K are shown for comparison. $z_{b,0}$ and h_0 are the corresponding values at $t = 0$ s. The h/h_0 data are adopted from Cheng *et al.*[3], where dashed lines are extrapolation as shown in **Supplementary Fig. 6**.

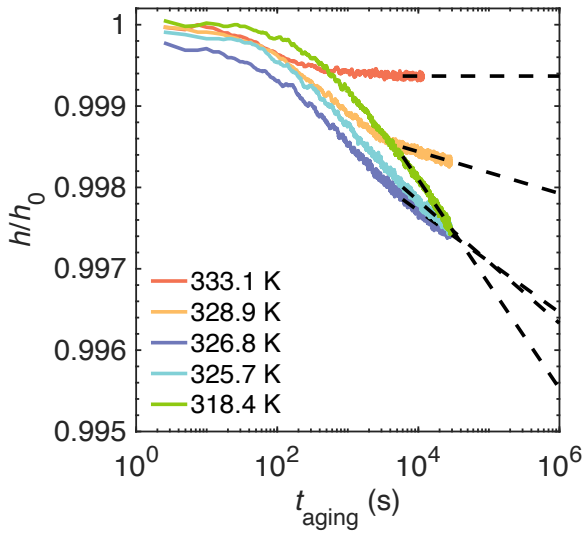

Supplementary Fig. 6 | Normalized thickness of 400-nm-thick LQG films vs. time during aging at various temperatures. h_0 is the film thickness at $t_{aging} = 0$ s. The data are adopted from Cheng *et al.*[3] Dashed lines are linear extrapolation in the logt_{aging} scale to the time window of our experiments.

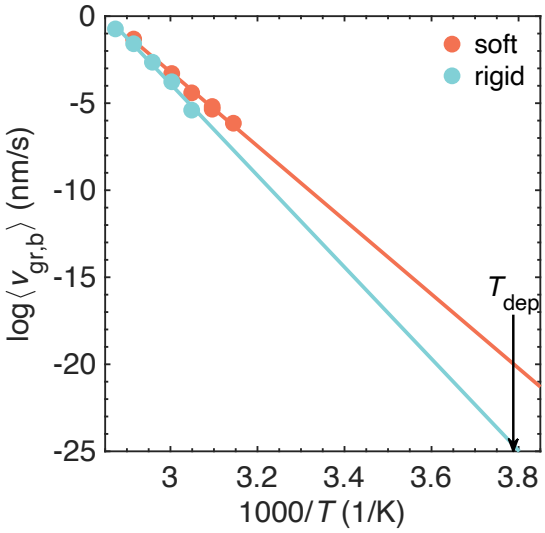

Supplementary Fig. 7 | Extrapolation of $\langle v_{gr,b}\rangle$ on soft and rigid substrates assuming Arrhenius temperature dependence. Black arrow denotes $T_{dep} = 264$ K. The derived activation energies are 407 ± 13 kJ/mol on soft substrate and 504 ± 31 kJ/mol on rigid substrate, respectively.

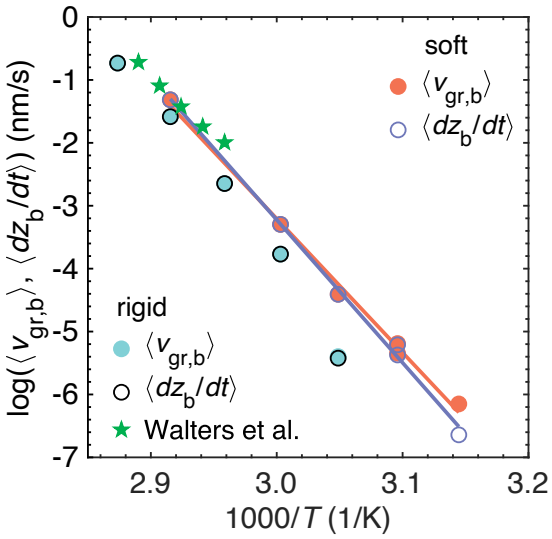

Supplementary Fig. 8 | Comparison between the front growth velocity associated with SG transformation, $\langle v_{\mathrm{gr,b}} \rangle$, and the upward moving velocity, $\langle dz_{\mathrm{b}}/dt \rangle$, of the buried SG/transformed-SCL interface in bilayer films prepared on soft and rigid substrates. Solid lines are linear fits to the $\langle v_{\mathrm{gr,b}} \rangle$ and $\langle dz_{\mathrm{b}}/dt \rangle$ data on soft substrates, revealing activation energies of 407 ± 13 kJ/mol (red) and 435 ± 13 kJ/mol (blue-violet), respectively. Green stars represent data adopted from Walter *et al.*[7] for single-layer TPD SGs deposited at $T_{\mathrm{dep}} = 260$ K on rigid substrates (silicon).

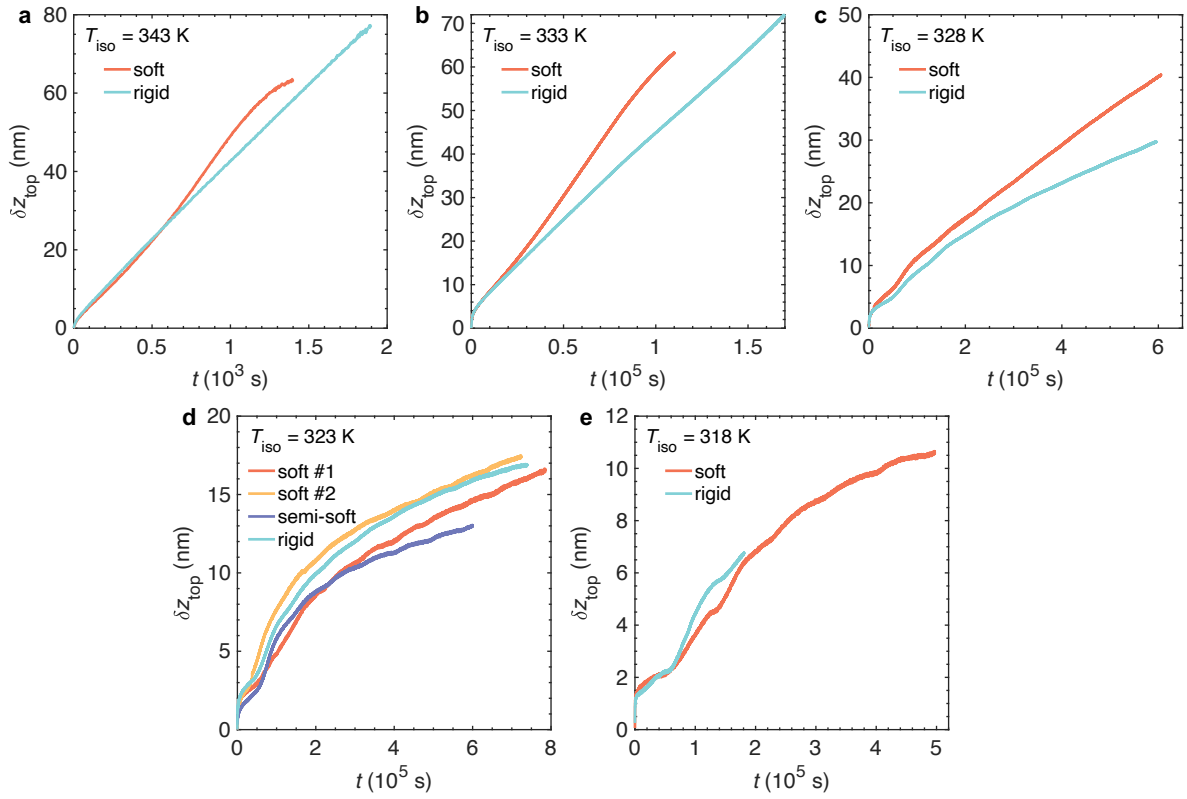

Supplementary Fig. 9 | Distance of top interface from the free surface, δz_{top}, vs. time during isothermal annealing at various T_{iso}: a, 343 K, **b**, 333 K, **c**, 328 K, **d**, 323 K, and **e**, 318 K. The data in **e** on rigid substrate is for a 180-nm-thick single-layer SG film, the rest in **a**-**e** are bilayers. The independent experiments were performed on soft substrates at $T_{iso} = 323$ K, labeled as #1 and #2.

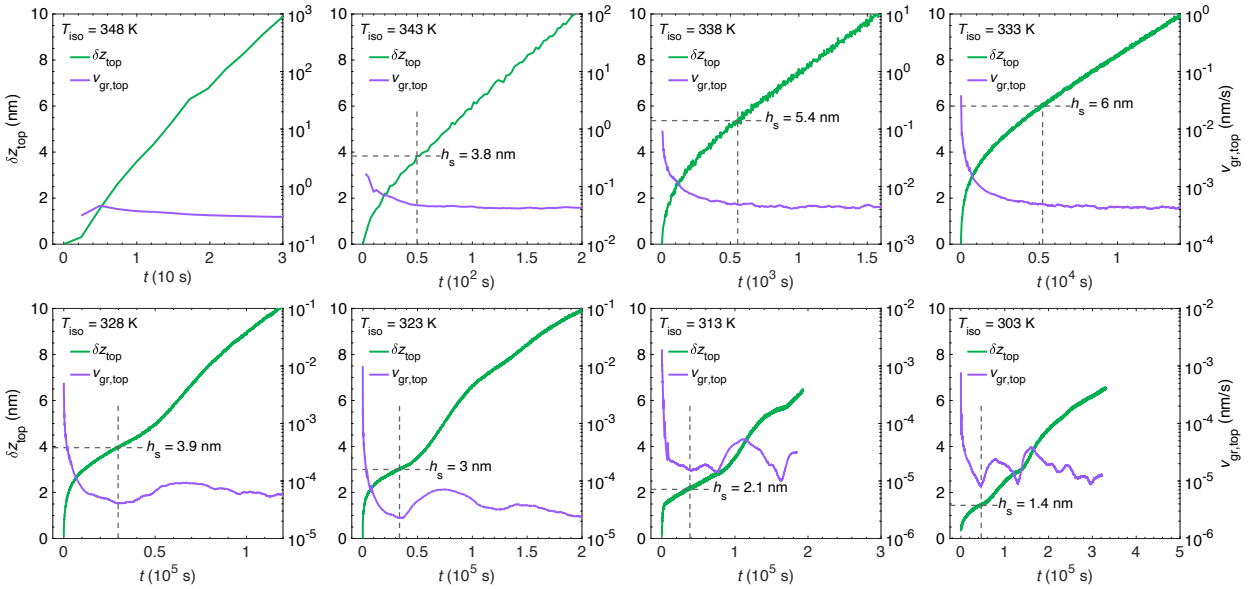

Supplementary Fig. 10 | Distance of top interface from the free surface, δz_{top}, and its corresponding instantaneous velocity, $v_{gr,top}$, vs. time for bilayer samples prepared on rigid substrates. Samples were isothermally annealed at various temperatures between 303 K and 348 K. The intersection of the horizontal and vertical dashed lines in the lower-T_{iso} plots ($\leq$ 343 K) marks the point where rapid changes in $v_{gr,top}$ end, defining the thickness of the mobile surface layer, h_s.

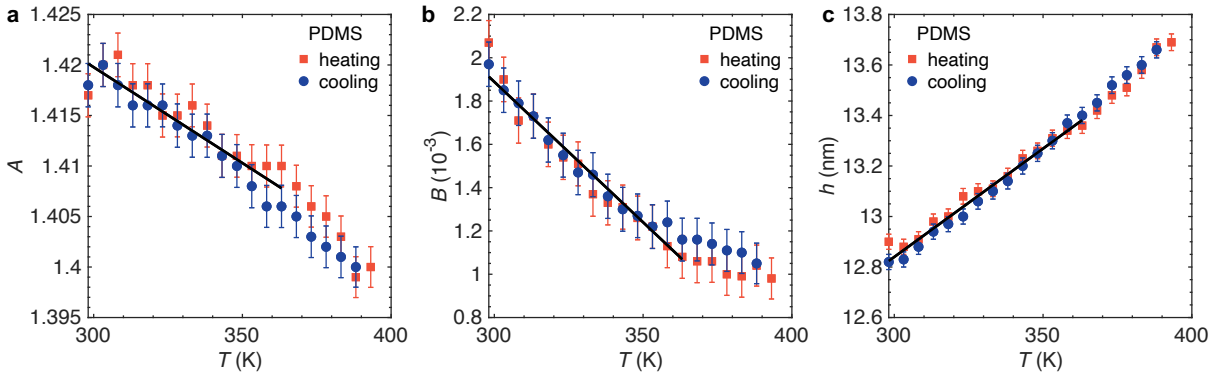

Supplementary Fig. 11 | Cauchy parameters of a 13-nm-thick PDMS film obtained by modeling the VASE data collected at various isothermal temperatures. Red squares represent the data obtained in heating from 298 K to 393 K at 10 K/min and with a 5 min isothermal hold at every 5 K interval. The blue circles are the data obtained upon subsequent cooling at the same rate, the same temperatures, and the same hold time. Error bars represent the 90% confidence intervals, calculated by the fit algorithm applied to the VASE data. Solid lines are a global linear fit to both data sets in the temperature range between 298 K and 363 K: **a**, $A = 1.4767 - 1.8967 \times 10^{-4} T$, **b**, $B = 5.7808 \times 10^{-3} - 1.2974 \times 10^{-5} T$, **c**, $h = 10.2658 + 8.5802 \times 10^{-3} T$, with thickness h in nm and temperature T in K.

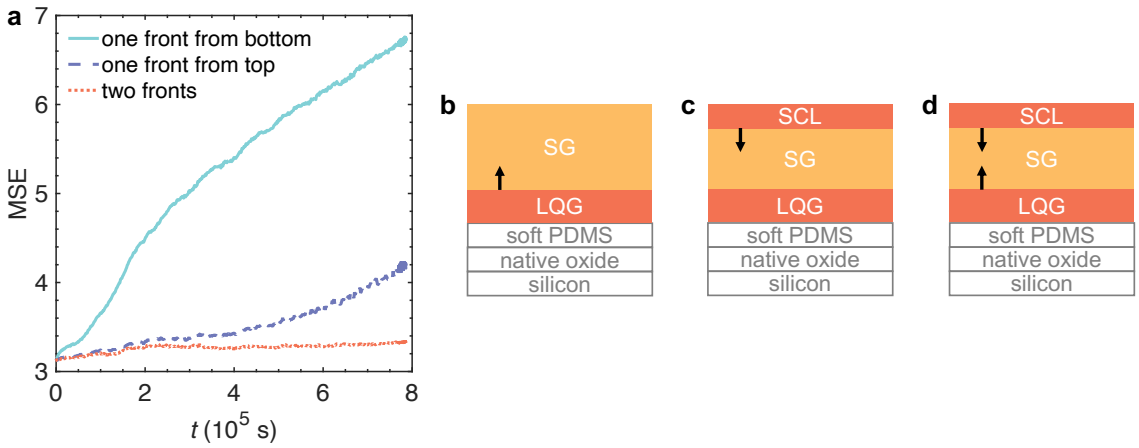

Supplementary Fig. 12 | Comparison between the mean square error (MSE) of various fitting models to the *in-situ* spectroscopic ellipsometry (SE) data. **a**, MSE vs. time during isothermal annealing of a bilayer on soft substrate at $T_{\text{iso}} = 323$ K. **b**-**d**, Schematic illustration of the models used for fitting: one transformation growth front originating from the SG/LQG (bottom) interface (**b**), one transformation growth front originating from the (top) free surface (**a**), and two transformation growth fronts at both interfaces (**d**). As seen in **a**, the model with two growth fronts (red) produces lower MSE than the other two models throughout the annealing experiment.

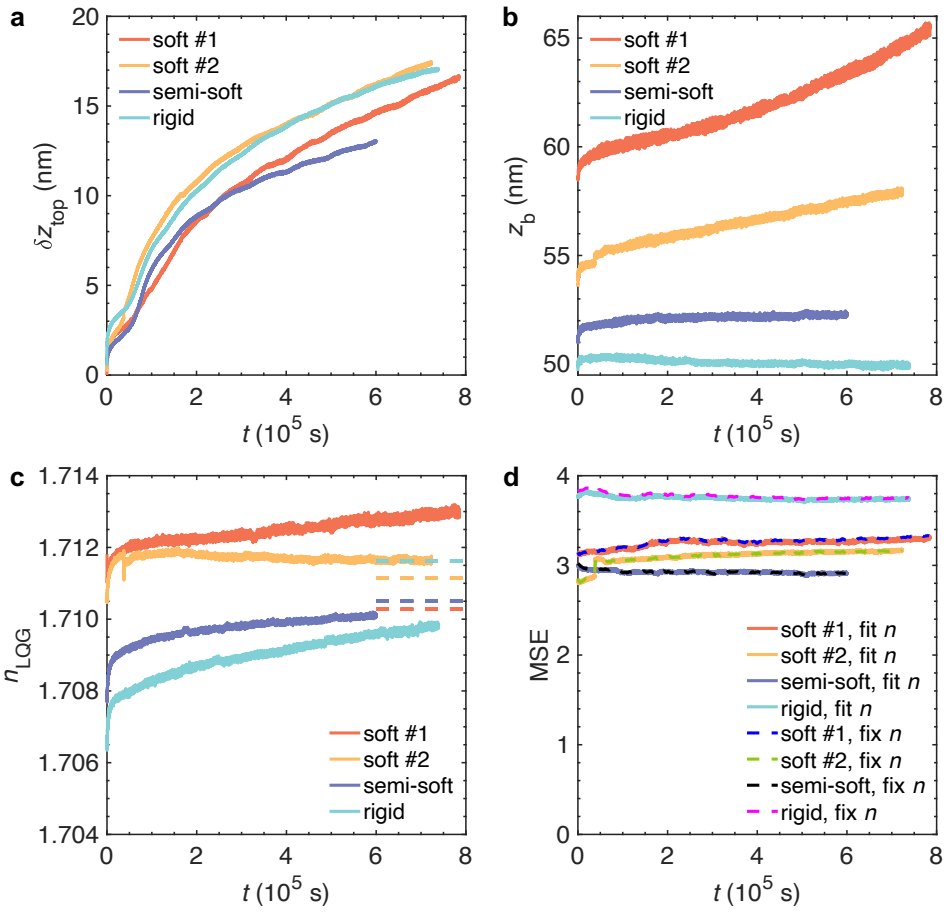

Supplementary Fig. 13 | Modeling of the *in-situ* spectroscopic ellipsometry (SE) data by treating the refractive index of the bottom LQG layer, n_{LQG}, as a fit parameter. **a**, Distance of top interface from the free surface, δz_{top}, **b**, position of the buried SG/LQG or SG/transformed-SCL interface, z_b, **c**, n_{LQG}, and **d**, MSE, vs. time during isothermal annealing at $T_{iso} = 323$ K, for bilayer samples on various substrates. Dashed lines in **c** indicate the n_{LQG} values of 180-nm-thick LQG films after full transformation of the bilayer and subsequent quenching to 323 K, following the same color scheme as the solid lines. Dashed lines in **d** correspond to the MSE of fittings with n_{LQG} fixed at the values as indicated by the dashed lines in **c**. The two independent trials on soft substrates were labeled as #1 and #2.

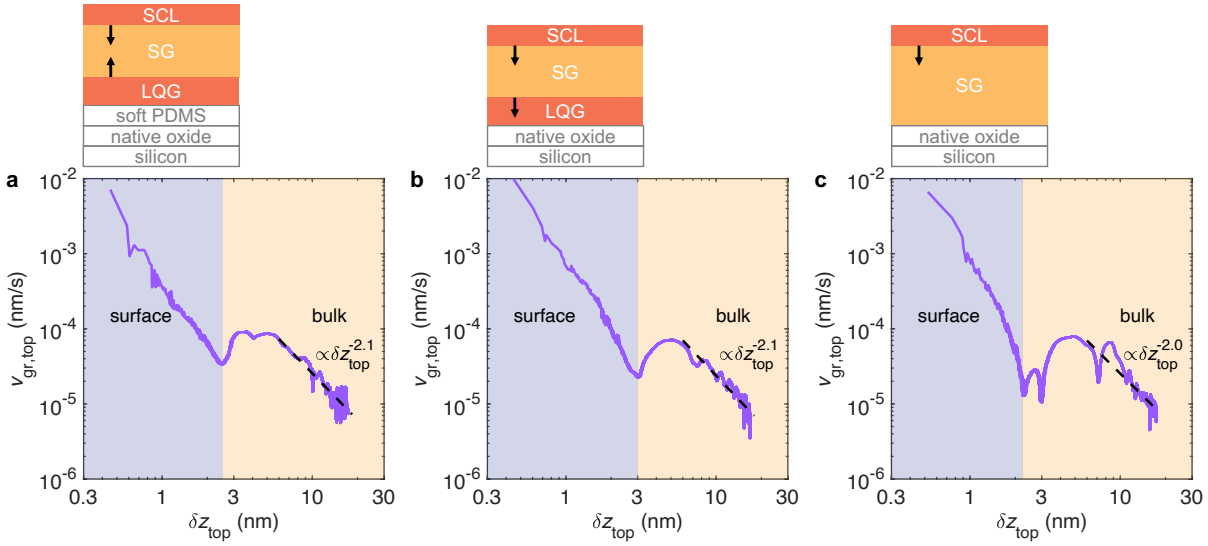

Supplementary Fig. 14 | Invariant surface dynamic gradient on bilayer and single-layer glasses on soft and rigid substrates. Instantaneous growth front velocity of the top interface, $v_{\mathrm{gr,top}}$ vs. the distance from the free surface, δz_{top}, during isothermal annealing at $T_{\mathrm{iso}} = 323$ K, for **a**,**b**, bilayer glasses on soft (**a**) and rigid (**b**) substrates, and **c**, a single-layer SG film on rigid substrate. Dashed lines represent power-law fit results: $v_{\mathrm{gr,top}} \propto \delta z_{\mathrm{top}}^{-2.1}$ (**a**,**b**), $v_{\mathrm{gr,top}} \propto \delta z_{\mathrm{top}}^{-2.0}$ (**c**). Blue-violet and orange shadings denote the mobile surface layer and the bulk region, respectively. Schematics above each plot illustrate the corresponding fitting models for the *in-situ* SE data, consisting of 6, 5, and 4 layers, respectively.

REFERENCES

1. McGuire, J. A., Merrill, J. H., Couturier, A. A., Thees, M. F. & Roth, C. B. Comparison of Physical Aging and Glass Transition in Glassy–Rubbery Polymer Bilayer Films. *The Journal of Physical Chemistry B* **129,** 2778–2788 (2025).

2. Rauscher, P. M., Pye, J. E., Baglay, R. R. & Roth, C. B. Effect of Adjacent Rubbery Layers on the Physical Aging of Glassy Polymers. *Macromolecules* **46,** 9806–9817 (2013).

3. Cheng, S. *et al.* Physical aging of glasses of an organic semiconductor. *Journal of Materials Chemistry C* **13,** 13214–13223 (2025).

4. Böttcher, C. J. F. & Bordewijk, P. *Theory of electric polarization* (Elsevier Science Limited, 1978).

5. Jin, Y. *et al.* Glasses denser than the supercooled liquid. *Proceedings of the National Academy of Sciences* **118,** e2100738118 (2021).

6. Luo, P. *et al.* High-density stable glasses formed on soft substrates. *Nature Materials* **23,** 688–694 (2024).

7. Walters, D. M., Richert, R. & Ediger, M. D. Thermal stability of vapor-deposited stable glasses of an organic semiconductor. *The Journal of Chemical Physics* **142,** 134504 (2015).